MATEC Web of Conferences **25**, 02006 (2015)
DOI: 10.1051/matecconf/20152502006

Effect of Second Phase Particles on Grain Growth for Nanocrystalline AZ31 Mg Alloy by Phase Field Methods

Yan Wu*
School of Mechanical Engineering, Wuhan Polytechnic University, Wuhan, Hubei, China

ABSTRACT: The grain growth of nanocrystalline AZ31 magnesium alloy containing spherical particles with different sizes is simulated by phase field methods. It is shown that the role of pinning effect of the second phase particles during grain growth is interesting. There is a critical particle size to affect the grain growth in nanostructure. If the size of particles is lower than the critical value, the effect of pinning for grain growth will be increased with further decreasing the size. If the size is larger than the critical value, the particles nearly have no pinning effects. The critical value is 200 nm when the content of particles is 10%. It is found that the grain growth exponents in kinetic equation decrease when the sizes of particles increase in nanostructure with the same volume fraction of the particles, and the pinning effect of particles on the grain growth is decreased as well.

Keywords: phase field methods; second phase particles; nanocrystalline structure; grain growth

1 INTRODUCTION

The moderate refinement of grains is an effective means to enhance the comprehensive properties of materials, and it is also the most important method to control the microstructure of materials, which has taken a lot of attentions of researchers [1, 2]. Dispersively distributed hard particles are usually used to make the grains smaller in matrix structure, due to their pinning force on grain boundaries to prevent the grain growth.

Phase field simulations have made some progress for studying the effect of second phase particles on the microstructure evolution at present [3-7]. Moelans et al. [4, 5] have presented a phase field model for the first time to simulate polycrystalline grain growth progress containing small incoherent second phase particles and to study the pining effect on microstructure evolution. Reference [6] has investigated the effect of particles with different shapes, volume fraction and sizes on two-phase grain growth by phase field method. Reference [7] has examined the effect of mobile second phase particles on the kinetics of polycrystalline grain growth using a phase field theory. However, these models are not in real time and space for real alloys. Our recently previous work has already achieved a phase-field model to simulate the grain growth process during recrystallization of AZ31 Mg alloy in real time and space, and the simulated results agree well with the experiments [8-12] by introducing a new concept of grain boundary range. It is believed that the model is for a grain growth simulation of realistic spatiotemporal evolution in nano and micron scale for the first time.

In this paper, we will build a phase field model to study the grain growth in nanocrystalline AZ31 Mg alloy containing second phase particles in the realistic spatiotemporal process, and examine the effect of second phase particles with different sizes on the nanostructure evolution and kinetics of grain growth for nanocrystalline AZ31 Mg alloy. The grain boundary range is studied between the grains, and the time exponents in the kinetic equation are investigated during the grain growth along the annealing time.

*Corresponding author: wuy611@163.com

2 PHASE FIELD MODEL CONTAINING SECOND PHASE PARTICLES

2.1 *Model fundamentals*

Phase field methods are based on thermodynamics and kinetics. The temporal evolution of microstructure can be determined by evaluating the time-dependent Allen-Cahn equation and Cahn-Hilliard diffusion equations as follows [13, 14]:

$$\frac{\partial \eta_p(\mathbf{r},t)}{\partial t} = -L\frac{\delta F}{\delta \eta_p(\mathbf{r},t)}, (p=1, 2, 3\ldots n)$$

$$\frac{\partial c(\mathbf{r},t)}{\partial t} = M\nabla^2\frac{\delta F}{\delta c(\mathbf{r},t)} \quad (1)$$

Where L and M are respectively the structural relaxation and chemical mobility parameters; $\eta_p(\mathbf{r}, t)$ is the long-rang orientation parameters and used to distinguish the different orientations of the grains; $c(\mathbf{r}, t)$ is a concentration field variable; p is the possible number of the grain orientations in the system, and it is taken as 32 as suggested in reference [15].

F is the free energy of the system, and its expression in isotropic single-phase system is seen as follows [15]:

$$F = \int_V [f_0(c,\eta_1(\mathbf{r},t),\eta_2(\mathbf{r},t),...,\eta_p(\mathbf{r},t)) + \frac{K_2}{2}\sum_{p=1}^{n}(\nabla\eta_p(\mathbf{r},t))^2]d\mathbf{r} \quad (2)$$

Where K_2 is the gradient energy coefficient and f_0 is the local free energy density function.

When the position and shapes of the second phase particles remain unchanged in the process of evolution , the local free energy density generated by the second phase particles is expressed as follows[4, 5]:

$$f_0^p = \varepsilon\varphi\sum_{p=1}^{n}\eta_p^2 \text{ , } (p=1, 2 \ldots n) \quad (3)$$

In this paper, the boundary energy between the particles and the matrix are not considered, so ε is chosen as 1[4, 5]. Φ is used to describe the distribution of the particles, when Φ=1, it means that there is a particle; when Φ= 0, it means that there is no particles; Φ is considered to be constant in time. The local free energy density of the system is described by the expression as follows:

$$f_0 = A + A_1(c(\mathbf{r},t)-c_l)^2 + \frac{A_2}{4}(c(\mathbf{r},t)-c_l)^4 - \frac{B_1}{2}(c(\mathbf{r},t)-c_l)^2\sum_{p=1}^{n}\eta_p^2(\mathbf{r},t) + \frac{B_2}{4}(\sum_{p=1}^{n}\eta_p^2)^2 + \frac{K_1}{2}\sum_{p=1}^{n}\sum_{p\neq q}^{n}\eta_p^2(\mathbf{r},t)\eta_q^2(\mathbf{r},t) + \varepsilon\varphi\sum_{p=1}^{n}\eta_p^2 \quad (4)$$

Where c_l is the concentration at the lowest point of the free energy curve as a function of concentration at a certain temperature, K_1 is the coefficient of coupling item between η_i and η_j.

If Φ=0, f_0 is minima when η_q^2=1 and $\sum_{p\neq q}^{n}\eta_p^2 = 0$. If Φ=1, f_0 is minima when $\sum_{p=1}^{n}\eta_p^2 = 0$.

2.2 *Grain boundary range among grains*

Magnesium alloys have caught great attentions in recent years for their high specific stiffness, high specific strength, low specific weight, and low pollution, but magnesium alloys have poor plasticity and strength. As we know, grain refining is a general way to improve both mechanical strength and ductility of metallic materials. Reference[16] is shown that a bulk nanocrystalline Al–5%Mg alloy revealed that it has four times the strength of a conventional Al-5083 alloy along with good ductility (8.5% elongation). In these simulations, AZ31 Mg alloy is chosen as the study material with the concentration of (in mass) w (Al) =3%, w (Zn) =1% with the rest of magnesium.

Reference[15] have claimed that the sharp-interface models were inappropriate for describing grains with sizes which are close to the boundary width, and the diffuse-interface field models have already been proposed to describe a polycrystalline microstructure by many orientation field variables[15,17-19]. In these models, grain boundaries are assumed to be diffuse with finite thickness, and its width is actually the range of field variables which is changed across the flat grain boundary. However, limited by the actual physical thickness of grain boundary thought as a few lattices parameters (for example 20Å), the parameters in the models were assumed as numerical values. Later, references [20-22] have produced an artificially diffuse interface at the length scale of practical interest. For example, increase the interface width from about 9nm to 36nm [21] without altering the kinetics and microstructure along the evolution path. However, the interface width is still too small for large grains on the order of micrometers and long time for hours in engineering scaling scope. In the phase field model of solidification, the interface thickness condition has also been discussed [23, 24], and Karma and so on have presented the thin-interface limit analyses, which allowed the width of diffuse interface to be larger than about an order of magnitude of the capillary length[23].

Therefore, we proposed a new concept called “grain boundary range” [9, 10] to define the distance of gradient variation of the long-rang orientation parameters across an interface. The “interfacial width” in phase field simulation should be optimally chosen to satisfy both precision and required computational efficiency so that our “grain boundary range” is the same as the interfacial width. However, "interfacial width" has another different meaning in material science that it is the geometrical width of an interface in a scope of 3-5 atom thickness. If we take the phase field “interfacial width” with the size of 3-5 atoms, the phase field simulation will has no any computational efficiency. We suggested that the phase field interfacial width can be as large as up to micrometers and we suggested a new term of “range” instead of width for clearance. Moreover, our study [9-10] finds that the range has a physical concept of the region around an interface which the interface affects in ways of interface energy and interfacial element segregation. The boundary energy of a low angle grain boundary, for example, is chiefly consistent of elastic strain energy, and it is formed by a series of dislocations of which their effective elastic field is in a size up to a micrometer. The position of the interface defined in our model is the geometric center of symmetry of the grain boundary range. The value of grain boundary range is 1.2 μm in microstructures [9], it is too large for grains in nano-scales whose grain size is less than 1μm and the grain boundary range will have no physical meaning if it covers more than two grains. The volume fraction of grain boundaries increases dramatically when the grain size decreases[25] and reference [26] showed that

the nanocrystalline materials might consist of over 50% of geometric boundary regions (interface component) depending on the average grain size. Therefore, we suggest that the nanocrystalline materials will have a grain boundary range which covers up to nearly two whole adjacent grains as seen in Figure 1.

Figure 1 is the variation of η across a flat boundary calculated by present model. It is already known from reference [9] that the values of η_j (j represents a certain orientation of the grains) varied in one grain from 1 to 0 into another grain are gradually across the grain boundary range. However, the grain boundary range covers its two adjacent grains in nano-scale in Figure 1, which means that the attribution of the orientation of a grain may be influenced not only by itself but also by its nearest neighbors. It is the size and the physical character of the boundary range that make the key difference in our present model for different scale applications.

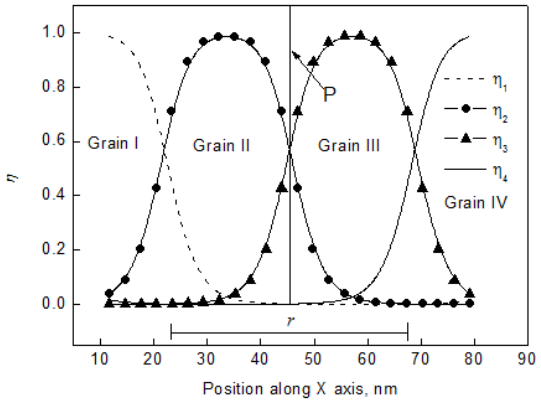

Figure 1. Characteristics of grain boundary in orientation parameters by simulations for nanoscale model: p — grain boundary position; r — the grain boundary range

Other parameters in Equation(2) in the model are already decided by our preliminary work for the study, and the research results have already been published in reference [12], the value of the parameters are as follows: c_l equals 0.2, A=-25.57 kJ/mol, A_1=99.14 kJ/mol, A_2=18.30kJ/mol, B_1=80.33kJ/mol, B_2=2321.51 kJ/mol, K_1=2090.16J/mol, K_2=0.21×10^{-13}J·m^2/mol[12].

2.3 *Nucleation condition*

The nucleation process of crystallization is simplified by a phenomenological method, and the well-defined microstructure is formed after a short time [20]. The initial state is given as the 4dx × 4dx unit grids which are evenly distributed in the simulated area, and the radius of the nucleus is a random value between 0 to 2 grids. There are two dimensional uniform grids which are 512×512 in the simulations. The overall size of the simulation cell is 1.5 μm×1.5 μm in nanostructure with each grid size of 2.93 nm, the local initial composition is considered as 0.03. The value of the time-step has to be relatively small in order to obtain the convergence results; however, an extremely small value of time-step will require more steps for solving the kinetic equations. The values of 0.6 seconds in the nano-scale model for time-steps are chosen to balance the two factors. The boundary condition of the differential equations is defined as the periodic boundary in order to minimize the boundary effect on the grain growth kinetics.

Considering the boundaries between the second phase particles and matrix are incoherent, and spherical particles are randomly introduced into the structures, the particles are shown as round in the two-dimensional conditions, so the total volume fraction occupied by the particles is expressed as f_p=2m（m+1）×N /W×100%, where m=[r/dx]; r is the particle radius, r=d/2; d is the particles diameter; dx is the size of unit grid; N is the number of particles; W is the total number of unit grid in the simulation. When the volume fractions are 10% in nanostructure, the diameter of particles is 30 nm, N is 438.

In the simulation, the particles with the diameters of 10 nm, 20 nm, 30 nm, 100 nm, 200 nm, 300 nm are introduced into the nanocrystalline AZ31 Mg alloy.

3 SIMULATION RESULTS

3.1 *Grain growth kinetics without the second phase particles*

Conventional grain coarsening in single phase polycrystalline materials is a migration process of grain boundaries; it is driven by the mean curvatures. Generally, it's thought to obey the parabolic kinetic equation, such as Hillert's theory [27] which predicted a time exponent n of the highly pure materials in grain growth as n=2, the equation is as follows:

$$D^n - D_0^n = kt \tag{5}$$

Where t is the evolution time; D is the average grain size in diameter; D_0 is the initial average grain size; k is a temperature dependent rate constant. However, the time exponent n is often deviated from the value 2 for practical reasons, reference [28] showed n = 5 for the grain growth in nanocrystalline AZ31 Mg alloy.

In order to check the reliability of the simulations, we have compared the simulated results of grain growth with the experimental results at different temperatures as shown in Figure 2.

It is seen that the simulated results are matched well with the experimental data at 300°C and 350°C. However, the simulated results are not matched very well with the experiments at 400°C in Figure 2, which may imply a different mechanism in activity energy at lower temperature. The grain growth is essentially obeyed the power law at n = 5 in Equation (5) in the process of grain growth.

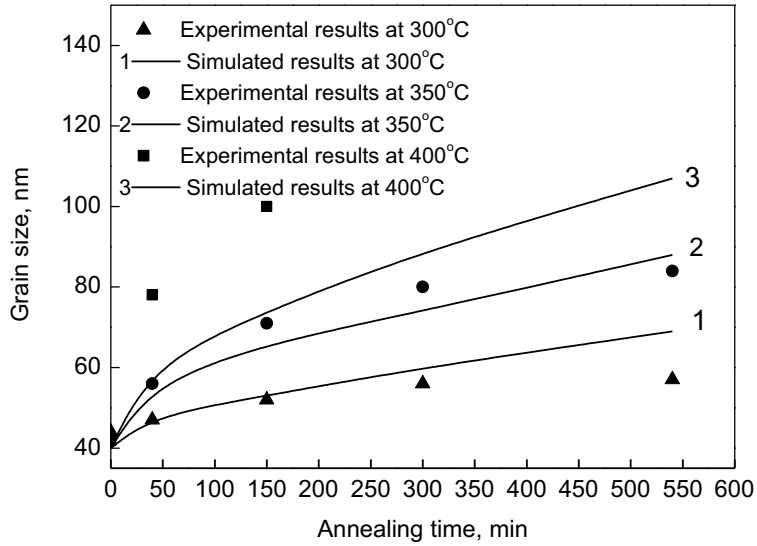

Figure 2. Simulated average grain size evolution as a function of annealing time compared with the experiments in reference [28] for nanocrystalline AZ31 Mg alloy at different temperatures.

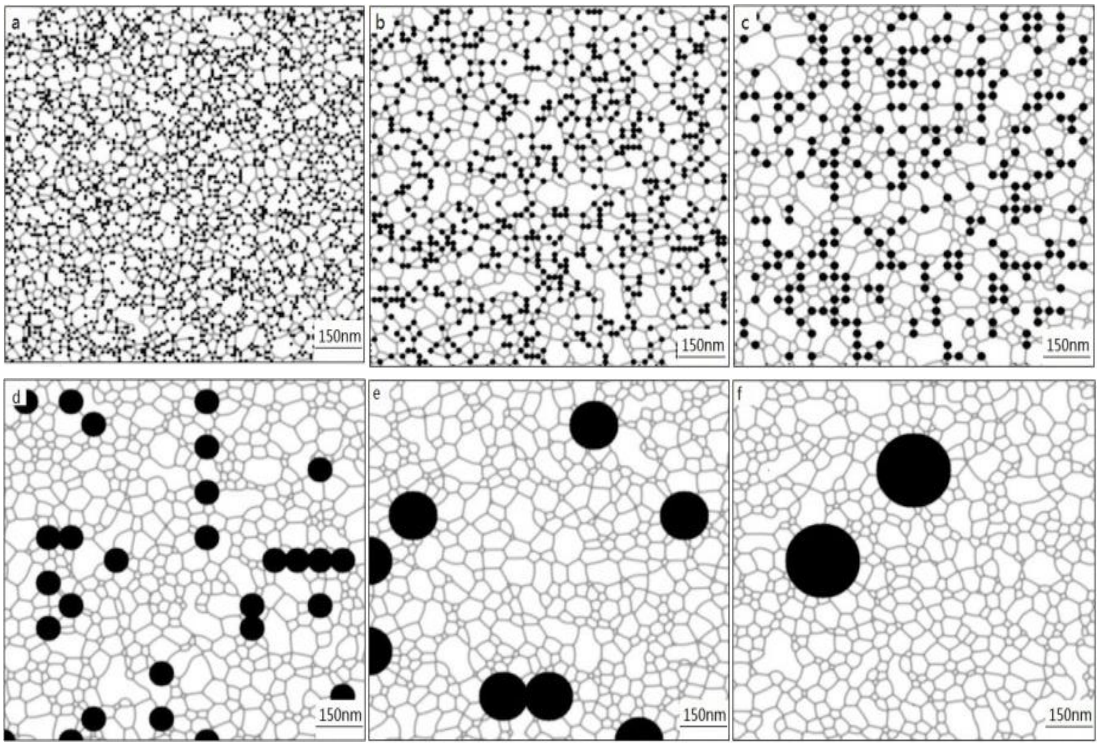

Figure 3. Simulated nano-strucutre with 10% of second phase particle for their diameter are respectively 10nm, 20nm, 30nm, 100nm, 200nm and 300nm when the annealing time is t=500 min with 350 ºC: (a) d=10nm, (b) d=20 nm, (c) d=30 nm, (d) d=100 nm, (e) d=200 nm, (f) d=300 nm.

3.2 *Effect of second phase particles with different sizes on nano-grain growth*

Two dimensional uniform grids of 512×512 are chosen in the models, and 10% of second phase particles are defined during nucleation in the nanostructure, the diameters are respectively 10 nm, 20 nm, 30 nm, 100 nm, 200 nm and 300 nm, the simulation results at 500min and 350oC are shown as Figure 3.

It is shown from Figure 3 that, some particles are inside the grains and some particles are at the grain boundaries when the size of particles is 10 nm. When their sizes are larger, more particles are at boundaries, which inform that the pinning effect of larger single particle is stronger for moving grain boundaries. From Figure 3 (a), (b), (c), (d), it is seen that the grain size is larger with larger particles when the anealing time is 500 min and the nanostructures contain the same volume fraction of particles, the phenomenon satisfies the law of Zener pinning.

When the volume fraction of the particles is 10%, the influence of different sizes on the grain growth for nanostructure AZ31 Mg alloy is investigated, and the simulated results are shown in Figure 4:

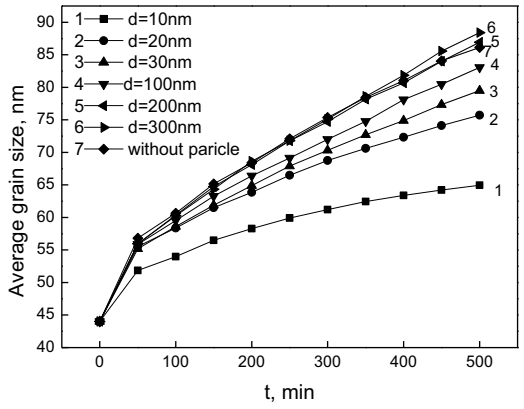

Figure 4. Changes of average grain sizes along with annealing time in nanostructure AZ31 Mg alloy containing 10% of the second phase particles with different sizes at 350 ºC

It is shown from Figure 4 that, the average grain size is increased along with the annealing time. However, the average grain size is decreased with further decreasing particle size at the same annealing time because when the particles fraction are the same, the smaller the particles, the more the number of particles, and the single grain boundary may be pinned by more small particles, which induces greater resistance of grain boundary moving and slower rate of grain growth. It has also been seen that, when the sizes of particles are 200nm and 300nm, the average grain size in nanostructure containing particles is close to that without particle, which means that there is a critical particle size of 200 nm to affect the grain growth in nanostructure when the particle volume fraction is 10%. If the particle size is smaller than 200 nm, the pinning effect on grain growth will be increased with further decreasing the particle size; if the size of particle is larger than 200 nm, the particles nearly have no pinning effect in the nanostructure AZ31 Mg alloy.

According to Figure 4, the grain growth exponents are investigated and the fitting results are shown in Table 1, where D is the average diameter of grains; n is the grain growth exponents; A and B are the parameters in the grain growth kinetic equation $D=A+Bt^{1/n}$.

It is seen from Table 1 that, when the particle size is increased from 10 nm to 300 nm, n is decreased from 9.0 to 5.3, which means the rate of grain growth is increased. When the second phase particle size is 200 nm, the parameters in the kinetic equations without particles or containing the second phase particles are much closed.

Table 1. Parameters in grain growth kinetic equation for different sizes of particles when the volume fraction is 10% in nanostructure at 350 ºC

Particle size(nm)	$D=A+Bt^{1/n}$		
	A	B	n
10	1.66	32.26	9.0
20	1.66	28.93	6.7
30	1.66	25.70	5.7
100	1.66	24.26	5.3
200	1.66	22.46	4.8
300	1.66	21.28	4.6
0	1.66	23.83	5.0

4 CONCLUSION

1. A phase field model is built to study the effect of second phase particles for nanocrystalline AZ31 Mg alloy, and the simulation results are compared with that without second phase particles.

2. It is found that the time exponent n in the kinetic equation is 5 in nanocrystalline AZ31 Mg ally without the second phase particles. These findings can be proved by limited experimental results found in the literature [28].

3. Simulated results showed that there is a critical particle size to affect the grain growth in nanostructure. If the size of particles is lower than the critical value, the effect of pinning for grain growth will be increased with further decreasing the size. If the size is larger than the critical value, the particles nearly have no pinning effect.

4. It is shown that the critical value is 200 nm when the content of particles is 10% in the nano-structural AZ31 Mg alloy.

5. It is found from simulation that the grain growth exponents in kinetic equation are decreased from 9.0 to 5.3 when the size of particles is increased from

10nm to 300nm in nanostructure and the volume fraction of particles is 10%, the pinning effect of particles on the grain growth is decreased as well.

ACKNOWLEDGEMENT

The authors acknowledge the National Nature Science Foundation of China (Grant No. 51171040 and No. 50771028), and National High Technology Research and Development Program of China (Grant No. 2013AA031601) for the financial support of this study.

REFERENCES

[1] Ali, Y. et al. 2015. Current Research Progress in Grain Refinement of Cast Magnesium Alloys: A Review Article. *Journal of Alloys and Compounds*, 619: 639-651.

[2] Svyetlichnyy, D. S. 2013. Modeling of Grain Refinement by Cellular Automata. *Computational Materials Science*. 77: 408-416.

[3] Fan, D. et al. 1998. Numerical Simulation of Zener Pinning with Growing Second-Phase Particles. *Journal of American Ceramic Society*. 81(3): 526-532.

[4] Moelans, N. et al. 2005. A Phase Field Model for the Simulation of Grain Growth in Materials Containing Finely Dispersed Incoherent Second-Phase Particles. *Acta Materialia* . 53: 1771-1781.

[5] Moelans, N. et al. 2006. Phase Field Simulations of Grain Growth in Two-Dimensional Systems Containing Finely Dispersed Second-phase Particles. *Acta Materialia*, 54: 1175-1184.

[6] Zhou, G. Z. et al. 2012. Phase-Field Method Simulation of the Effect of Hard Particles with Different shapes on Two-Phase Grain Growth. *Acta Metallurgica Sinica*. 48 (2): 227-234.

[7] Mallick, A. 2013. Effect of Second Phase Mobile Particles on Polycrystalline Grain Growth: A Phase-Feld Approch. *Computational Materials Science*. 67: 27-34.

[8] Zong, Y. et al. 2009. Phase Field Simulation on Recrystallization and Secondary phase precipitation under Strain Field. *Acta Physica Sinica*. 58: S161-08.

[9] Wang, M. T. et al. 2009. Grain Growth in AZ31 Mg Alloy during Recrystallization at Different Temperatures by Phase Field Simulation. *Computational Materials Science*. 45: 217-222.

[10] Zhang, X. G. et al. 2011. A Physical Model to Express Grain Boundaries in Grain Growth Simulation by Phase-Field Mrthod . *Acta Physica Sinica*. 60(6): 068201-1-9

[11] Zhang, X. G. et al. 2012. A Model for Releasing of Stored Energy and Microstructure Evolution during Recrystallization by Phase-Field Simulation. *Acta Physica Sinica.* 61(8): 088104-1-9.

[12] Wu, Y. et al. 2013. Grain growth in multiple scales of polycrystalline AZ31 magnesium alloy by phase field simulation. *Metallurgical and Materials Transactions A*. 44 A(3): 1599-1610.

[13] Allen, S. M. et al. 1979. A Microscopic Theory for Antiphase Boundary Motion and Its Application to Antiphase Domain Coarsening. *Acta Metallurgica*. 27 (6): 1085-1095.

[14] Cahn, J. W. & Hilliard, J. E. 1958. Free Energy of a Nonuniform System. I. Interfacial Free Energy. *The Journal of Chemical Physics*. 28(2): 258-267.

[15] Fan, D. et al. 1997. Computer Simulation of Grain Growth Using a Continnum Field Model. *Acta Materialia*. 45: 611-622.

[16] Youssef, K. R. et al. 2006. Nanocrystalline Al-Mg Alloy With Ultrahigh Strength and Good Ductility. *Scripta Materialia*. 54(2): 251-256.

[17] Kazaryan, A. et al. Grain growth in systems with anisotropic boundary mobility: Analytical model and computer simulation. *Physical Review B.* 63(18): 184102-184102.

[18] Wen, Y. et al. 2003. Phase-field modeling of bimodal particle size distributions during continuous cooling. *Acta Materialia*. 51(4): 1123-1132.

[19] Kim, S. G. et al. 2006. Computer simulations of two-dimensional and three-dimensional ideal grain growth. *Physical Review E*. 74(6): 061605-1-14.

[20] Chen, Q. et al. 2004. Quantitative phase field modeling of diffusion-controlled precipitate growth and dissolution in Ti-Al-V. *Scripta Materialia*. 50(4): 471-476.

[21] Shen, C. et al. 2004. Increasing length scale of quantitative phase field modeling of concurrent growth and coarsening processes. *Scripta Materialia*. .50(7): 1029-1034.

[22] Wen, Y. H. B. et al. 2006. A Phase-Field Model for Heat Treatment Applications in Ni-based Alloys. *Acta Materialia*. 54 (8): 2087-2099.

[23] Karma, A. & Rappel, W. J. 1998. Quantitative phase-field modeling of dendritic growth in two and three dimensions. *Physical Review E*. 57 (4): 4323-4349.

[24] Kim, S.G. et al. 1998. Interfacial compositions of solid and liquid in a phase-field model with finite interface thickness for isothermal solidification in binary alloys. *Physical Review B*. 58(3): 3316-3322.

[25] Nishizawa, T. 2006. *Thermodynamics of Microstructure*. In S. M. Hao (ed.). Beijing: Chemical Industry Press,.

[26] Shek, C. et al. 1999. Grain growth in nanocrystalline SnO2 prepared by sol-gel route. *Nanostructured Materials.* 11(7): 887-893.

[27] Hillert, M. 1965. On the theory of normal and abnormal grain growth. *Acta Metallurgica.* 13(3): 227-238.

[28] Deng, C. 2009. *Fabrication of Ulter-fine Grain Magnesium Alloy by Powder Metallurgy and Research on the Microstructure and Property*. Harbin Institute of Technology: Harbin.